

Accounts

Physical Chemistry of the Lowest Excited Singlet State of *trans*-Stilbene in Solution as Studied by Time-Resolved Raman Spectroscopy

Hiro-o Hamaguchi* **and Koichi Iwata**

Department of Chemistry and Research Centre for Spectrochemistry, School of Science, The University of Tokyo, 7-3-1 Hongo, Bunkyo-ku, Tokyo 113-0033

(Received November 20, 2001)

Structure and dynamics of the lowest excited singlet state of *trans*-stilbene (the S_1 state of *t*SB) in solution are discussed with an emphasis placed on the elucidation of the mechanism of the *trans–cis* photoisomerization. Structure of S_1 *t*SB in solution is first discussed based on the time-resolved Raman spectral data and their isotope substitution effects. Original data for an asymmetrically deuteriated *t*SB, *t*SB-d_5, are presented to confirm the ethylene-like structure of the central C–C linkage of S_1 *t*SB. Next, the time-, temperature-, and solvent-dependent band shape changes of the olefinic C=C stretch band are discussed in terms of the solvent induced dynamic polarization. It is shown that the dynamic polarization model accounts very well, not only for the observed band shape changes, but also for their relevance to the isomerization mechanism. A new microscopic view on the photoisomerization of *t*SB is thus presented. Picosecond energy dissipation process of S_1 *t*SB is then discussed in relation to the microscopic solvation structure in chloroform. Finally, the mechanism of a new bimolecular reaction between S_1 *t*SB and carbon tetrachloride is discussed on the basis of the diffusion-controlled reaction model.

The *cis–trans* photoisomerization of olefins is one of the simplest chemical reactions that can be initiated by light. Using ultrashort laser pulses for photoexcitation and probing, we are now able to trace the whole process of photoisomerization by various time-resolved spectroscopies. Unprecedented opportunities of *looking at a reaction in its real time-course* are now open to us. *trans*-Stilbene is a prototype olefin that exhibits its photoisomerization. Both the *trans* and the *cis* isomers of stilbene (*t*SB and *c*SB) are stable in the ground state and no interconversion takes place at room temperature. Photoexcitation of *t*SB with near-ultraviolet light results in the formation of *c*SB with a quantum yield of about 0.5. This photoisomerization of *t*SB is known to proceed via the lowest excited singlet (S_1) state.[1] Being the key intermediate of photoisomerization, S_1 *t*SB has been stimulating the field of time-resolved spectroscopy continuously for both the electronic and the vibrational degrees of freedom. The isomerization kinetics of S_1 *t*SB can be studied directly by time-resolved fluorescence spectroscopy. Since the isomerization rate in the S_1 state is much larger than the radiative decay rate and the rates of the other non-radiative decay processes, the observed fluorescence decay rate is approximately equal to the rate of isomerization. Numerous time-resolved fluorescence studies were thus performed in the last two decades for S_1 *t*SB in a wide range of environments, from the isolated molecule in a supersonic jet to the solvated molecules in polar and non-polar solvents. These studies were already collected in two comprehensive reviews.[2,3] Briefly summarizing, the observed temperature-dependent rates of isomerization were fit to the Arrhenius-type formula to give the frequency factors (pre-exponential factors), which then, were interpreted in terms of various statistical models. The RRKM model was most often used for the isolated molecule and the Kramers model and its modifications were the choice for the solvated molecules.[3] The results indicate that the agreement between the experiment and theory is not global. In particular, the marked solvent dependence of the S_1 *t*SB isomerization is yet to be elucidated on new experimental and theoretical bases. Meanwhile, the present authors concentrated on Raman spectroscopy of S_1 *t*SB in solution in order to look at the photoisomerization process from the viewpoint of structural chemistry. As is well established, Raman spectroscopy is the most sensitive structural probe of short-lived intermediate species in solution.[4–6] Any correlation between the isomerization dynamics and the molecular structure is likely to be manifested in the Raman spectrum. In the present Account, we focus on our time-resolved Raman spectroscopic investigations of S_1 *t*SB in solution. The primary objective is to introduce a structural perspective of the S_1 *t*SB photoisomerization. Two other topics related to S_1 *t*SB, the solvent/solute interaction and the new photochemistry with carbon tetrachloride are also included.

Raman spectroscopy of S_1 *t*SB started in the year 1983,

when two independent papers were published simultaneously. The Standard Oil group in the US (Gustafson et al.) used a high repetition-rate amplified dye laser system to obtain a picosecond transient Raman spectrum of S_1 *t*SB in hexane.[7] The Tokyo group (Hamaguchi et al.) used low repetition-rate (10 Hz) nanosecond lasers and observed the same S_1 Raman spectrum of *t*SB in hexane.[8] The latter work demonstrated that Raman spectroscopy of a picosecond-lived excited state was still possible using nanosecond lasers, provided that the pump peak power was sufficiently high to ensure a detectable population of the excited state. After these papers were published, S_1 *t*SB has been repeatedly studied by many groups using transient and time-resolved (spontaneous and coherent) Raman spectroscopy.[9–49] There is a good reason why S_1 *t*SB is chosen. The strong $S_1 \leftarrow S_0$ absorption of *t*SB is located in the near ultraviolet region and an even stronger $S_n \leftarrow S_1$ absorption band lies around 600 nm. These locations of absorptions facilitate a convenient experimental set-up in which the second harmonic (~300 nm) of a picosecond dye laser is used for photoexcitation, while the fundamental (~600 nm) is used for probing resonance Raman scattering from the S_1 state. Furthermore, S_1 *t*SB is not too strongly fluorescent in the wavelength region near 600 nm, where Raman scattering is to be detected. The early transient Raman works were devoted to establishing the vibrational assignments of S_1 *t*SB through the use of the isotopic substitution technique. Structure of S_1 *t*SB was thus characterized on the basis of these vibrational assignments.[5] Then, the focus moved to the ultrafast time-dependent spectral changes which had been predicted from the probe-laser power dependence of the nanosecond transient Raman spectrum.[14] It was only in 1992, ten years after the first demonstration of the S_1 *t*SB transient Raman spectrum, that the predicted time dependence was actually observed by real picosecond time-resolved experiments.[21,22] The discovery of this ultrafast phenomenon led many researchers to go further into the Raman spectroscopy of S_1 *t*SB. More recent studies measure the time-resolved Raman spectra in the anti-Stokes region to obtain information on the vibrational relaxation dynamics. The analysis of the Raman excitation profiles by Nakabayashi, Okamoto, and Tasumi has shown that the vibrational relaxation of S_1 *t*SB is very fast so that the $v = 1$ state of the olefinic C=C stretch vibration is formed within a few picoseconds after the photoexcitation.[42] Transient and time-resolved Raman studies have also been extended to *trans*-stilbene in the lowest-excited triplet state.[50,51]

The presently accepted view on the stilbene photoisomerization is based on the adiabatic potential curves schematically shown in Fig. 1.[52] In the ground electronic state (S_0), there is a large potential barrier separating *t*SB and *c*SB. The two ground-state isomers are therefore stable and are not interchangeable with each other at room temperature. The excited singlet potential curve has a deep minimum at the (90 degree twisted) *perpendicular* configuration and shallow minima at the *trans* and *cis* configurations. The barrier to the *trans-perpendicular* rotation is reported to be 2–4 kcal mol^{-1} depending on the solvent and is significantly higher than that to the *cis-perpendicular* rotation (at most 1 kcal mol^{-1}). If S_0 *t*SB is photoexcited in solution, vibrationally-relaxed S_1 *t*SB is formed in 10–20 picoseconds (see the discussion below). It is

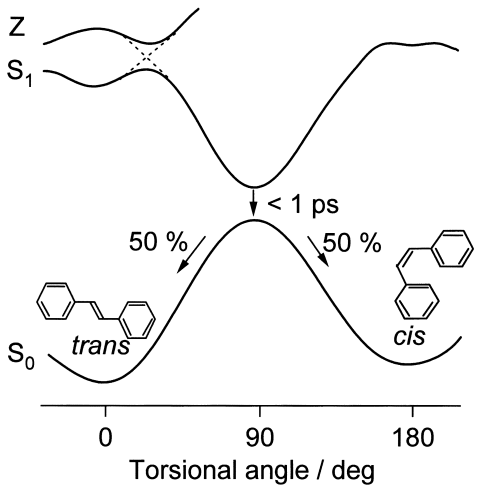

Fig. 1. Schematic diagram of the adiabatic potential curves accounting for the stilbene photoisomerization.

then thermally activated to go over the barrier in 30–100 ps time scale to generate a *perpendicular* singlet state, which is internally converted very rapidly (< 1 ps) to the ground-state with the same *perpendicular* configuration. Thus, the *trans* to *perpendicular* isomerization serves as the simplest model for the thermally activated reaction process. On the ground-state potential curve, the *perpendicular* configuration relaxes to the *trans* and *cis* configurations with nearly a 50/50 ratio. This scheme explains the observed photoisomerization quantum yield close to 0.5. The barrier to the *trans-perpendicular* rotation was first explained theoretically in terms of an avoided crossing between the π–π^* S_1 state, which has a potential minimum at the *trans* configuration, and a higher-lying singlet state, called here the Z state, which has a potential minimum at the *perpendicular* configuration.[53] Since then, the electronic structure of *t*SB in the lowest excited singlet manifold and its relevance to the isomerization mechanism has been an issue in quantum chemistry.[54] Here, we do not go into the details of these quantum chemical studies but note that the Z state is likely to be a highly polar zwitterionic state.[55,56] The *cis* to *trans* isomerization is thought to proceed in a similar way via the perpendicular singlet state. In this *cis* case, the isomerization rate is much larger than that of the *trans*, because of a much lower barrier to the internal rotation.

Raman Spectra and Structure of S_1 *t*SB in Solution

The first step for elucidating the *t*SB photoisomerization is to establish the structure of the key intermediate, S_1 *t*SB. Raman spectrum has so far been the only source of information on the structure of S_1 *t*SB in solution. A representative Raman spectrum of S_1 *t*SB in heptane is shown in Fig. 2. More than fifteen Raman bands are observed with high S/N ratios. The vibrational assignments of these bands were carried out through the use of isotopic frequency shifts.[5] The results are listed in Table 1, together with the ^{13}C shift values reported by Gustafson et al.[15] The primary concern here is the vibrational assignments of the olefinic vibrations and the structural information coming therefrom. There are three Raman-active olefinic vibrations to be considered; the central C=C stretch vibra-

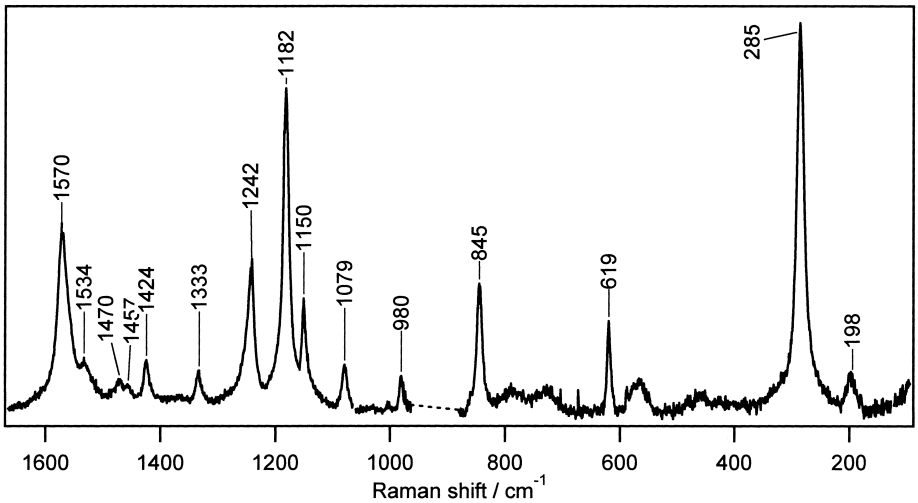

Fig. 2. Transient Raman spectrum of S_1 *trans*-stilbene measured at 50 ps after the photoexcitation in heptane. Pump and probe wavelengths are 294 nm and 588 nm.

Table 1. Observed Raman Shifts of S_1 *trans*-Stilbene and S_1 *trans*-Stilbene-^{13}C, and Their Mode Assignments

Raman shift/ cm^{-1}		Assignment[a),c)]
S_1 *trans*-stilbene[a)]	S_1 α,α'-^{13}C-*trans*-stilbene[b)]	
1570	1521	olefinic C=C str
1534	1545	ring str
1470		ring str
1457		ring str
1424	1418	ring str
1333	1331	ring str + CH def
1242	1236	olefinic CH def
1182	1144	C-Ph str
1150	1169	ring CH def + C–Ph str
1079	1075	ring CH def
980	976	trigonal + breath
845	834	ring def + C=C–C def
619	620	ring def
285	287	C–C_0 def
198	194	C=C–C def

a) Present study in heptane. b) Ref. 15. c) Ref. 57.

tion, the symmetric C–Cph stretch vibration, and the symmetric C–H in-plane bend vibration. They are all characterized by their sensitivity to the ^{13}C substitution of the olefinic carbons. In the Raman spectrum displayed in Fig. 2, a strong band is observed at 1570 cm^{-1}. As is shown later, this band shows significant shifts of the peak position depending on time, solvent, and temperature and is therefore called the "$\sim$1570 cm^{-1} band" in the following. The $\sim$1570 cm^{-1} band shows a large ^{13}C shift of 45 cm^{-1}, which is 74% of the theoretical ^{13}C shift for the pure C=C stretch. It is therefore assigned to the olefinic C=C stretch vibration. The bands at 1242, 1182, 1150, and 845 cm^{-1} show small but significant ^{13}C shifts (5–10 cm^{-1}) and are assigned to the vibrational modes that have contributions from the three olefinic vibrations. All the other bands showing no or much less ^{13}C shifts are safely assigned to the ring vibrations.

Normal coordinate analyses have been carried out by different groups using empirical[57] as well as quantum-chemical force fields.[58,59] They all show that the three olefinic vibrations mix significantly with one another and that the magnitude of mixing depends strongly on the force field. Due to the lack of a reliable force field, however, the details of these mode mixings still remain unclear and the experimental vibrational assignments in Table 1 have not been fully supported by normal coordinate analysis. In fact, a recent quantum chemical calculation by Negri et al.[59] has suggested a drastic change of the structure of *t*SB on going from the S_0 to the S_1 state. According to their calculation, the central part of S_1 *t*SB is not ethylene-like but somewhat butadiene-like rather; the calculated C–Cph bond length (1.403 Å) is shorter than the C=C length (1.493) in the S_1 state. Such calculated structural changes have led Negri et al. to assign the $\sim$1570 cm^{-1} band to the C–Cph stretch vibration which is supposed to be a double bond according to their calculation. This assignment, however, is not

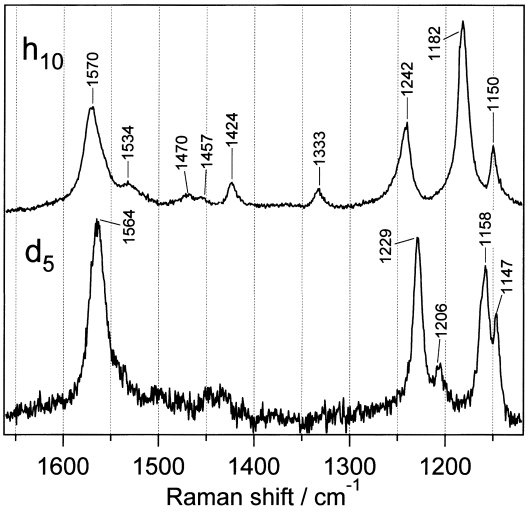

Fig. 3. Transient Raman spectrum of S_1 *trans*-stilbene (upper trace) and S_1 *trans*-stilbene-d_5 (lower trace) measured at 50 ps after the photoexcitation in heptane.

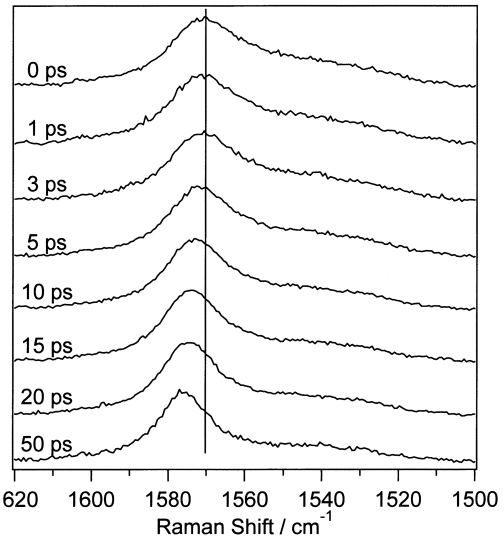

Fig. 4. Time dependence of the ~1570 cm^{-1} band of S_1 *trans*-stilbene measured in chloroform. Delay time for each trace is shown in the figure.

compatible with our new Raman data on an asymmetrically substituted *t*SB, *t*SB-d_5, in which one of the two phenyl rings is deuteriated. In *t*SB-d_5, there are two different C–Cph bonds, C–Cph-d_0 and C–Cph-d_5 and hence two different C–Cph stretch frequencies. A Raman band contributed significantly by the C–Cph stretch vibration should show a splitting or, at least, a broadening on going from *t*SB to *t*SB-d_5. As shown in Fig. 3, the ~1570 cm^{-1} band of S_1 *t*SB does not show either a splitting or a broadening. In stead, the three Raman bands near 1200 cm^{-1} change markedly on going from the normal *t*SB to *t*SB-d_5. From these observations we conclude that the C–Cph stretch mode does not contribute significantly to the ~1570 cm^{-1} band and that its contribution is distributed among the three vibrations located around 1200 cm^{-1}. The assignment of the ~1570 cm^{-1} band to the C=C stretch vibration is thus strongly supported. Considering the fact that the frequency ~1570 cm^{-1} falls in the frequency region of a C=C double bond, we conclude that S_1 *t*SB has an *ethylene-like structure* with a slightly reduced C=C bond order. Note that the C=C stretch frequency in the S_0 state is 1639 cm^{-1}. The frequency decrease of 70 cm^{-1} on going from S_0 to S_1 is significant but not large enough to rationalize the rotation around the C=C bond in the S_1 state.

Analysis of the Time- and Solvent-Dependent Raman Spectral Changes of S_1 *t*SB

Time-Dependent Raman Spectral Changes and Vibrational Cooling. The time-dependent Raman spectral changes of S_1 *t*SB in chloroform are shown in Fig. 4. As the delay time between the pump and probe pulses increases, the peak position of the ~1570 cm^{-1} band shifts to higher frequency and, concomitantly, the bandwidth decreases. A similar change is found also for the 1180 cm^{-1} band, though in a much less magnitude (not shown in Fig. 4). These time-dependent spectral changes were first predicted from the probe-power dependence of the nanosecond transient Raman spectra (optical depletion timing) and were ascribed to the formation of "hot" S_1 *t*SB by photoexcitation.[14] Time-resolved Raman measurements by Hester et al.[25] and Qian et al.[26] have confirmed that the spectral changes are in fact due to the vibrational cooling of photogenerated "hot" S_1 *t*SB. Figure 5 compares the delay-time dependence of the peak position of the ~1570 cm^{-1} band and the observed anti-Stokes/Stokes intensity ratio of the 285 cm^{-1} band, which is proportional to the temperature.[38] The time dependence of the peak position agrees very well with that of the temperature, indicating that the peak position changes linearly with temperature.

Why does the ~1570 cm^{-1} (C=C stretch) band of S_1 *t*SB change with temperature? A naive answer to this question would be to assume the contributions from the hot transitions (inhomogeneous broadening). At higher temperatures, many low-frequency modes of S_1 *t*SB are thermally excited and, if the C=C stretch vibration is anharmonically coupled with

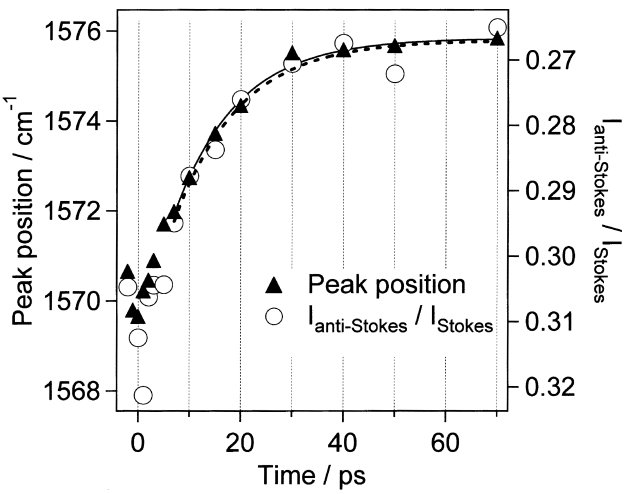

Fig. 5. Time dependence of the peak position of the ~1570 cm^{-1} band (filled triangles, left axis) and the anti-Stokes/Stokes intensity ratio of the 285 cm^{-1} band (open circles, right axis) of S_1 *trans*-stilbene in chloroform.

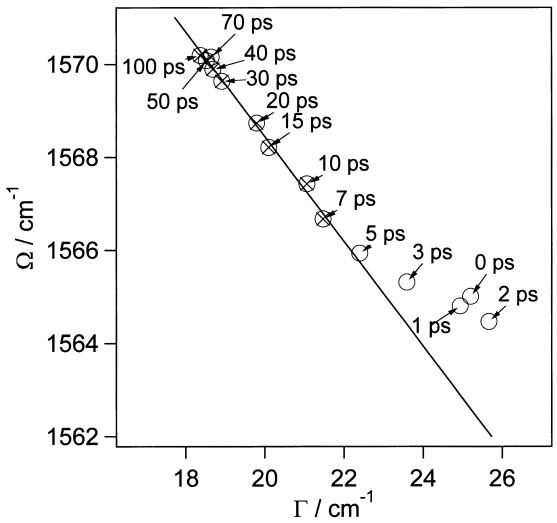

Fig. 6. Relationship between the peak position (Ω) and the bandwidth (Γ) of the ~1570 cm^{-1} band of S_1 *trans*-stilbene measured in heptane at various delay times. Delay time for each point is indicated in the figure. Data points marked with crosses are those used for least squares fitting analysis. The result of the fitting is shown with a solid line.

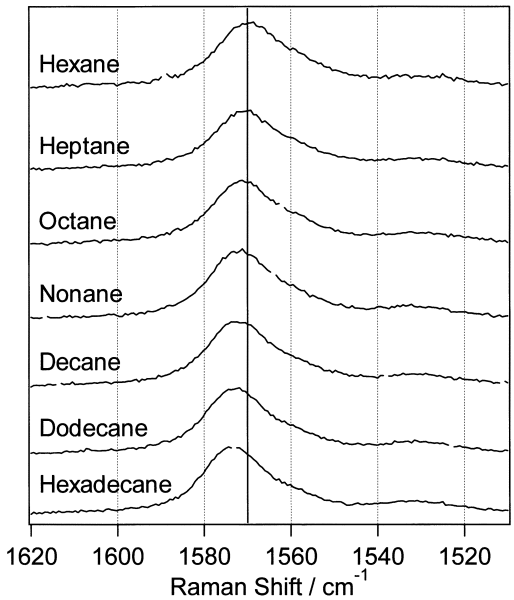

Fig. 7. Solvent dependence of the ~1570 cm^{-1} band of S_1 *trans*-stilbene measured at 50 ps. Used solvent for each trace is indicated in the figure.

these low-frequency modes, the ~1570 cm^{-1} band shape may well change with temperature, reflecting the distributed frequencies of the hot transitions. A detailed band-shape analysis, however, has indicated that the shape of the C=C stretch band of S_1 *t*SB is always a Lorentzian, regardless of the delay time and therefore regardless of temperature. It is unlikely that the frequency distribution of the hot transitions is *always accidentally* a Lorentzian. The Lorentzian band shapes are more in harmony with a homogeneous broadening mechanism. A least-squares fitting analysis using a Lorentzian function gives precise values of the peak position Ω and the bandwidth Γ of the C=C stretch Raman band at a certain delay time. The Ω and Γ values thus determined for 14 delay times are plotted in Fig. 6. The plot shows that a linear relationship holds between these two quantities. It is likely that the deviation from the linear relationship, observed between 0 ps and 5 ps, is caused by the temporally overlapping pump electromagnetic field, which affects both the position and width of the S_1 *t*SB Raman bands including the ~1570 cm^{-1} band.[49] Such a linear relationship between Ω and Γ is also obtained in a wider temperature range from the results reported by Hester et al.[25] This unexpected linear relationship between Ω and Γ led the present authors to set up a new model to account for the observed temperature dependence of the S_1 *t*SB Raman spectrum.

Solvent-Dependent Raman Spectral Changes and the *trans-perpendicular* Isomerization. As mentioned earlier, the rate of *trans-perpendicular* isomerization of S_1 *t*SB depends strongly on the solvent. If there is any manifestation of the isomerization dynamics in the observed Raman spectrum of S_1 *t*SB, it should be solvent-dependent. We therefore examined the solvent dependence of the S_1 Raman spectra in detail both in alkane solutions[24] and in alcohol solutions.[60] In both classes of solvents, marked changes were found for the C=C stretch band. Figure 7 shows the change of the C=C band shape in seven different alkanes. A monotonic up-shift of the peak position and a less clear but meaningful band narrowing are concomitantly observed on going from hexane to hexadecane. These spectral changes are found to be very similar to the temperature-dependent changes described above in the sense that the band shape is always a Lorentzian and that a Ω–Γ linear relationship holds. It seems that the time- and solvent-dependent C=C band shape changes of S_1 *t*SB originate from the same molecular mechanism.

It has also been found that the observed solvent-dependent spectral changes are correlated very closely with the isomerization dynamics. Figure 8 shows a plot of the observed peak

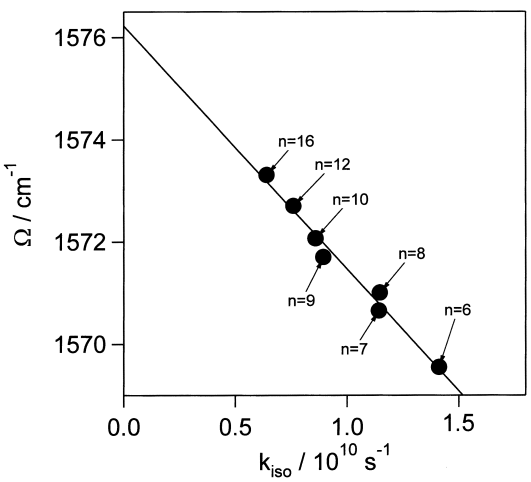

Fig. 8. Relationship between the peak position (Ω) of the ~1570 cm^{-1} band and *trans-perpendicular* isomerization rate constant (k_{iso}) of S_1 *trans*-stilbene measured in various normal alkane solvents. Number of carbon atoms in alkane molecules for each data point is shown in the figure.

position Ω against the rate of isomerization k_{iso} which was determined separately by picosecond time-resolved fluorescence spectroscopy. We see a clear linear relationship between Ω and k_{iso}. A similar linear relationship should hold between Γ and k_{iso} because Ω is linearly correlated with Γ. This Ω–k_{iso} (or Γ–k_{iso}) linear relationship is totally unexpected; there is no obvious reason why the peak position (= vibrational frequency) Ω or the bandwidth Γ should be linearly correlated with the rate of isomerization k_{iso}. If we extrapolate the Ω–k_{iso} (or Γ–k_{iso}) linear relationship to $k_{iso} = 0$, we obtain the intrinsic values of Ω (or Γ) which should be regarded as the peak position (or bandwidth) that is not affected by the isomerization dynamics. By using these intrinsic values of the peak position and the bandwidth, we can convert the observed Ω and Γ values to the change of the peak position $\Delta\Omega$ and the increase in the bandwidth $\Delta\Gamma$. The $\Delta\Omega$ and $\Delta\Gamma$ values then represent the "net" effect of the isomerization dynamics on the shape of the C=C Raman band. Note that the linear relationship between Ω and Γ is transferred to that between $\Delta\Omega$ and $\Delta\Gamma$. The Ω–k_{iso} (or Γ–k_{iso}) relationship is transferred to the $\Delta\Omega$–k_{iso} (or $\Delta\Gamma$–k_{iso}) relationship as well.

Solvent-Induced Dynamic Polarization, Vibrational Dephasing, and the C=C Stretch Band Shape. We now consider theoretically the two newly observed features of the C=C Raman band shape changes of S_1 *t*SB in solution. 1) The change of the peak position $\Delta\Omega$ and the increase in the bandwidth $\Delta\Gamma$ are correlated with each other making a linear $\Delta\Omega$–$\Delta\Gamma$ relationship. This is true for both the temperature- and solvent-dependent changes. 2) The band shape changes are correlated with the isomerization dynamics. A linear $\Delta\Omega$–k_{iso} (or $\Delta\Gamma$–k_{iso}) relationship has been obtained.

The isomerization dynamics is most likely to be related to the interaction of the S_1 state with the nearby Z state (see Fig. 1). How can the C=C stretch frequency of S_1 *t*SB be correlated with the interaction with the Z state? Or how can the vibrational dephasing (band width) of the C=C stretch mode be correlated with the interaction with the Z state? We have proposed a model based on the idea that the C=C stretch frequency is stochastically modulated by the time-dependent polarization of the S_1 state (termed *dynamic polarization*). According to this model, the fluctuation of the solvent field affects the energy gap between the S_1 and Z states and hence the Z state is occasionally mixed into the S_1 state by time-dependent perturbation. The C=C stretch angular frequency then changes stochastically between the two limiting values, the C=C double-bond angular frequency ω_1 in the S_1 state and the C–C single-bond angular frequency ω_2 in the Z state ($\omega_1 > \omega_2$). Both the short-range Lennard-Jones type interaction and the long-range Coulombic interaction are likely to cause the dynamic polarization.

In the following, we first adopt the simplest model in which the C=C angular frequency hops to and fro between ω_1 and ω_2. The Raman band shape corresponding to this two-frequency exchange dynamics was formulated first by Anderson[61] and later by Shelby et al.[62] and Hamaguchi[63] using different approaches. We assume that the forward (ω_1 to ω_2) hopping rate W_1 is much smaller than the backward (ω_2 to ω_1) hopping rate W_2 and, at the same time, W_1 is much smaller than the absolute value of the angular frequency difference $|\delta\omega| = |\omega_2 - \omega_1|$. In this asymmetric exchange limit, which we believe is the case with S_1 *t*SB in solution, the C=C angular frequency stays at ω_1 for most of the time and it occasionally hops to ω_2 but comes back very quickly to ω_1 (Fig. 9). In other words, the *t*SB molecule is in the S_1 state for most of the time and it occasionally hops to the Z state but it returns to the S_1 state very quickly because of the very short duration of the collision. The second condition, $W_1 << |\delta\omega|$ or $|\delta\omega|/W_1 >> 1$, means that the hop from ω_1 to ω_2 occurs only occasionally so that there is no relation between any two consecutive hops. The band shape in this limit is given by a Lorentzian with a shift of the peak position Ω and an increase in the bandwidth Γ from the unperturbed C=C stretch band shape;[63]

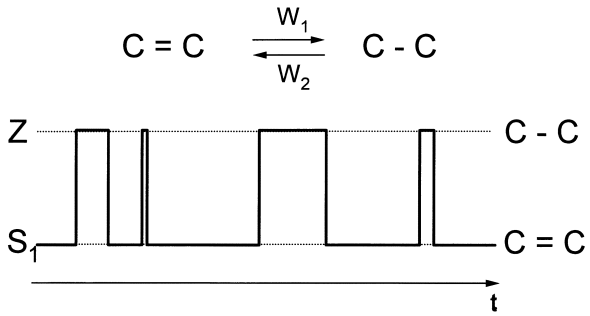

Fig. 9. Schematic diagram for the exchange between the C–C stretching frequency (ω_1) and the C–C stretching frequency (ω_2) caused by solvent induced dynamic polarization between the S_1 state and the Z state.

$$\Delta\Omega = W_1\tau/(1 + \tau^2), \quad (1)$$

$$\Delta\Gamma = W_1\tau^2/(1 + \tau^2), \quad (2)$$

where $\tau = \delta\omega/W_2$ represents the mean phase shift for one hop. Note that $1/W_2$ is the mean time that *t*SB stays in the Z state and the product of this mean time with the angular frequency difference $\delta\omega$ makes the mean phase shift for a hop. A large τ value ($|\tau| >> 1$) means that there is no phase memory after a hop. For this case, Eqs. 1 and 2 give $\Delta\Omega = 0$, $\Delta\Gamma = W_1$, in agreement with the ordinary collision-broadened band shape theory. Note that W_1 corresponds to the collision frequency in the gas phase experiment. For $\tau = 0$, we have no effect of the hop as expected. For $|\tau| < \sim 1$, $\Delta\Omega$ and $\Delta\Gamma$ are the functions of two quantities W_1 and τ and they satisfy the relation $\Delta\Gamma = \tau\Delta\Omega$. This relation indicates that, under a condition where the mean phase shift τ is regarded as constant, a linear relationship holds between the change of the peak position $\Delta\Omega$ and the increase in the bandwidth $\Delta\Gamma$.

Inversely, the observed linear relationship between $\Delta\Omega$ and $\Delta\Gamma$ of S_1 *trans*-stilbene can be considered to be a consequence of the constant mean phase shift τ for both the temperature- and solvent-dependent changes under our experimental conditions. It is likely that, in a small temperature range, the characteristics of the solute–solvent interaction do not change much except for the frequency of solvent fluctuation that corresponds to W_1. We can assume that the mean phase shift τ stays constant, while the forward hopping rate W_1 increases with increasing temperature. Equations 1 and 2 then account for the

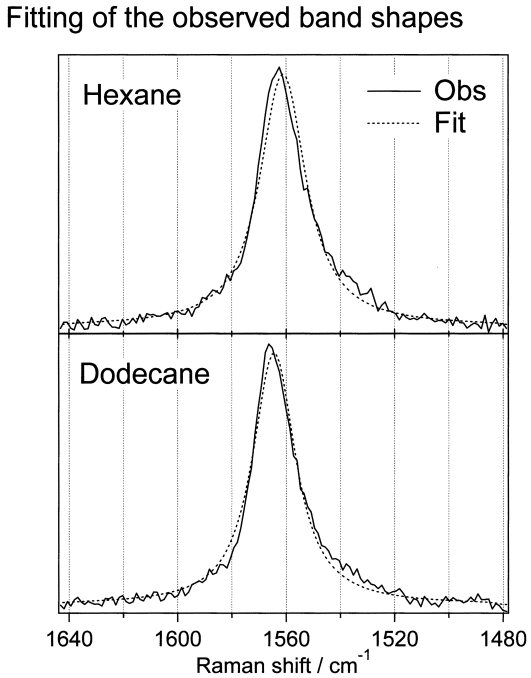

Fig. 10. The ~1570 cm^{-1} band of S_1 *trans*-stilbene-d_{10} in hexane (upper trace) and in dodecane (lower trace). Observed bands are shown with solid traces while bands simulated by the dynamic polarization model are shown with dotted traces.

observed down shift of the peak position ($\Delta\Omega < 0$) and the increase in the bandwidth ($\Delta\Gamma > 0$) of the C=C stretch Raman band of S_1 *t*SB with increasing temperature. It is also expected that, in a class of like solvents, the frequency of solvent fluctuation is the primary quantity that changes and the other characteristics of the interaction remain the same. The fluctuation frequency is expected to increase with decreasing viscosity or on going from a small solvent to a large one. Then, on going from a short alkane to a long alkane, W_1 is expected to decrease. Equations 1 and 2 again account well for the observed down shift ($\Delta\Omega < 0$) and the band width increase ($\Delta\Gamma > 0$) with increasing the chain length of the alkane solvent. The experimentally determined value of τ is slightly different for alkanes and for alcohols. For alkanes, $\tau = -0.31$[24] and -0.36[37] were obtained for S_1 *t*SB and S_1 *t*SB-d_{10}, respectively. More recent experiments for three alkanes, hexane, octane, and decane, at five different temperatures gave $\tau = -0.35$.[64] A larger value, $\tau = -0.45$, was obtained for S_1 *t*SB in alcohols.[60] It seems reasonable that the τ value is larger in polar solvents than in nonpolar solvents, because the polar environments are likely to stabilize the Z state and lengthen the duration of one hop (a smaller value of W_2), leading to a larger value of the mean phase shift for a hop.

By using the dynamic polarization model, we can interpret the solvent dependent change of the ~1570 cm^{-1} Raman bands very well. In this analysis, we use *t*SB-d_{10} rather than *t*SB-h_{10}. A ring mode is observed at 1534 cm^{-1} in the Raman spectrum of S_1 *t*SB-h_{10} as a shoulder of the ~1570 cm^{-1} band (see Figs. 2 and 3). This band is downshifted in S_1 *t*SB-d_{10} leaving the ~1570 cm^{-1} band isolated and more suitable for the band shape analysis. The unperturbed C=C stretch frequency, ω_1, is determined by the extrapolation of the observed Ω values to $k_{iso} = 0$. In the case of S_1 *t*SB-d_{10} in alkanes, $\omega_1 = 1568$ cm^{-1} is obtained.[37] By taking the difference, we can convert Ω to $\Delta\Omega = \Omega - \omega_1$. By introducing the $\Delta\Omega$ and τ (−0.36) values into Eq. 1, we obtain the forward hopping rate W_1 for each solvent. The W_1 value thus determined is 2.7×10^{12} s^{-1} ($(370\ fs)^{-1}$) in hexane and 1.5×10^{12} s^{-1} ($(670\ fs)^{-1}$) in dodecane. These values seem to be physically reasonable, since our recent molecular dynamics/quantum chemical approach[65] has shown that the solvent fluctuation causing the dynamic polarization of acetone in acetonitrile occurs with a frequency of a few hundred fs^{-1}. By using these W_1 and τ values, we can reproduce the observed band shapes of the C=C stretch Raman bands in hexane and dodecane as shown in Fig. 10. The solvent dependent Raman spectral changes of S_1 *t*SB are thus very well interpreted in terms of Eqs. 1 and 2. The temperature-dependent band shape changes of the ~1570 cm^{-1} band are also interpreted very well in the same way.

Solvent-Induced Dynamic Polarization and the *trans to Perpendicular* Isomerization Dynamics

By using Eq. 1, the observed Ω–k_{iso} linear relationship can be converted to the more "foreseeable" k_{iso}–W_1 linear relationship,

$$k_{iso} = W_1 P(T), \tag{3}$$

where $P(T)$ is the temperature dependent coefficient and T is temperature. For S_1 *t*SB in seven alkanes at 300 K, $P(300) = (3.2 \pm 1.2)\times10^2$ has been obtained.[24] Recent temperature dependent experiments in three alkanes have given $P(T)$ values ranging from 2.8×10^2 (283 K) to 3.8×10^2 (313 K).[64] These $P(T)$ values mean that one in about three hundred solvent fluctuations is effective in rotating the C–C bond, resulting in the *trans to perpendicular* isomerization.

Equation 3 has a formulaic resemblance with the Arrhenius formula,

$$k_{iso} = A\exp(-\Delta E/RT), \tag{4}$$

where A is the frequency factor and ΔE is the activation energy and R is the gas constant. The activation energy for the isomerization in shorter normal alkanes has been determined from the isoviscocity plot of k_{iso} vs temperature as 3.5 kcal mol^{-1}.[66,67] If we convert $P(300) = (3.2 \pm 1.2)\times10^2$ to an exponential factor, $\exp(-\Delta E'/RT)$, with $T = 300$ K, we obtain $\Delta E' = 3.4 \pm 0.3$ kcal mol^{-1}. Thus, there is a numerical agreement between Eq. 3 and the Arrhenius formula. In other words, information on the frequency factor A for the *trans to perpendicular* isomerization of S_1 *t*SB is obtained from the analysis of the dephasing kinetics of the olefinic C=C stretch mode. Generally speaking, we can think of a vibration, *reaction mode*, which is involved directly in the course of a reaction and without whose dephasing the reaction can never proceed. The reaction mode may well be a vibration that has a significant amplitude along the reaction coordinate so that the coherence of the vibration must be lost when the reaction is initiated. It is then not surprising if there is a correlation be-

tween the reaction rate and the rate of dephasing of such a mode. The C=C stretch mode of S_1 *t*SB provides the most obvious and the most illuminating example of the reaction mode. Recently, we extended the treatment of dynamic polarization from the two-frequency exchange model to the more general case of the continuous frequency modulation.[64] We showed that the key results of the two-frequency exchange model can also be obtained for the continuous frequency modulation model.

The formulaic resemblance and the numerical agreement between Eqs. 3 and 4 indicate that (3) is as meaningful as (4) in describing the chemical reaction kinetics. The Arrhenius formula (4) does not tell much about the microscopic details of the reaction. On the other hand, Eq. 3 shows us that the isomerization reaction of S_1 *trans*-stilbene is triggered by the solvent induced dynamic polarization of the C=C bond and that such a polarization occurs once in a few to ten hundred femtoseconds on an average in alkane solvents at room temperature, with one in about 300 of those polarizations eventually leading to the isomerization. Equation 3 is complementary to the Arrhenius formula (4) in the sense that it provides a detailed molecular-level view on the process of chemical reactions in solution.

The dynamic polarization model of photoisomerization is a working hypothesis to account for the newly observed relationship between the isomerization rate and the Raman spectral changes of S_1 *t*SB in solution. It needs more experimental support as well as theoretical sophistication before it is accepted as a general model.

Solvent/Solute Interaction as Revealed by Energy Dissipation Kinetics

As shown in Fig. 5, the peak position of the $\sim$1570 cm^{-1} Raman band of S_1 *t*SB changes linearly with temperature. This correlation is further confirmed by plotting the peak position observed at the delay time of 50 ps, when the time dependent spectral change is over, against the temperature of the bulk solution. The plot for the chloroform solution is given in Fig. 11,

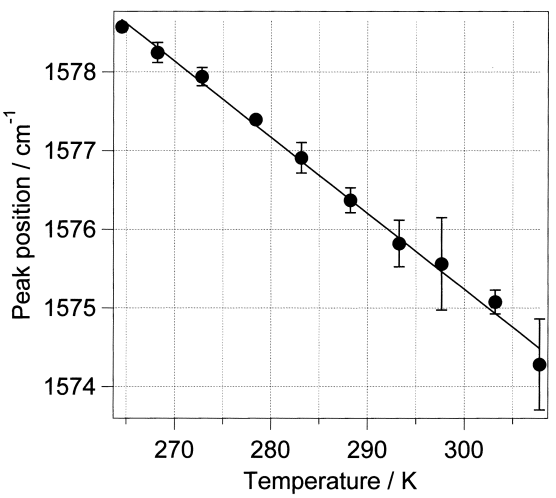

Fig. 11. Temperature dependence of the peak position of the $\sim$1570 cm^{-1} band of S_1 *trans*-stilbene measured at 50 ps in chloroform.

which shows that the linear relationship holds between 265 and 308 K. The same linear relationship has been reported by Hester et al.,[25] although there is quantitative difference between the two results. Linear relationships have also been obtained for hexane between 271 and 318 K, for octane between 268 and 332 K, for decane between 269 and 348 K,[64] and for SDS micellar solution between 294 and 328 K.[43] On the basis of this linear relationship, we can determine the temperature of S_1 *t*SB by measuring the peak position of the $\sim$1570 cm^{-1} band. Note that it is much easier and more reliable to measure the peak position than to measure the anti-Stokes/Stokes intensity ratio. Since we can determine the temperature with picosecond time resolution, we now have a "picosecond Raman thermometer".

When a molecule is photoexcited with more energy than needed for the 0–0 excitation, the excess energy is deposited to the vibrational degrees of freedom. As the excess energy is dissipated into the surroundings, the molecule cools down. If the molecule is solved in solution, the dissipated excess energy has to be transferred to the nearby solvent molecules. It is known that the excess energy generated in the course of a chemical reaction is removed by the surrounding molecules quite effectively in solution. This quenching process plays an important role in controlling the reaction, by stabilizing the reaction products and preventing the back reaction and/or further undesired reactions from occurring. The situation is quite different in chemical reactions in the gas phase where the excess energy is preserved in the hot product molecules unless they collide with other molecules. It is therefore important to clarify the mechanism of intermolecular energy transfer in solution so as to fully understand and control the chemical reaction process in solution. By measuring the cooling kinetics of a solute molecule by the "picosecond Raman thermometer", we can monitor the solute-solvent energy transfer process.

From the observed time dependence of the peak position of the $\sim$1570 cm^{-1} band (Fig. 5), it is concluded that S_1 *t*SB cools down in approximately 10 ps in chloroform. In this experiment, the amount of excess energy given to S_1 *t*SB upon the photoexcitation is 2800 cm^{-1}. What does this cooling time of 10 ps mean? We have measured the cooling curves of S_1 *t*SB in a number of solvents and found that the cooling kinetics has a strong correlation with the temperature diffusivity of the solvent. For example, the temperature diffusivity of ethylene glycol is 9.75×10^{-8} m^2 s^{-1} while that of chloroform is 8.22×10^{-8} m^2 s^{-1}.[68] The time dependent changes of the peak position of the $\sim$1570 cm^{-1} band in these two solvents clearly show that the cooling rate in ethylene glycol is larger than that in chloroform (Fig. 12). By fitting these curves with single exponential functions, we obtain the cooling time constants of S_1 *t*SB as 6.7 ps for ethylene glycol and 13 ps for chloroform. The cooling rates of S_1 *t*SB obtained in this way are plotted against the temperature diffusivity for 10 solvents in Fig. 13.[38] Strong correlation between the cooling rate and temperature diffusivity is obvious in this figure. However, temperature diffusivity is a bulk property of the solvent while the cooling rate reflects the rate of population decay of vibrationally excited states. Why are these two quantities correlated with each other? In order to answer this question, we assume the following mechanism for the excess energy dissipation process. When

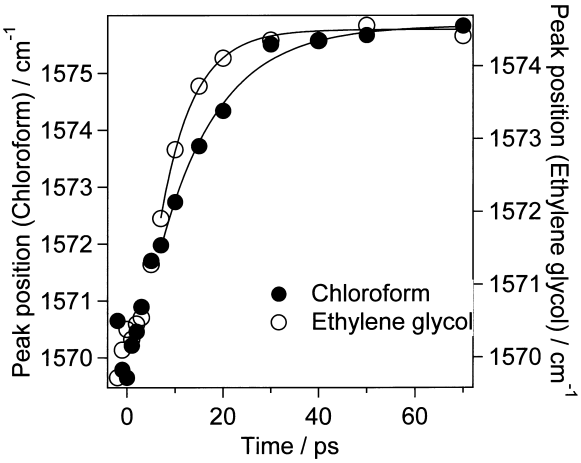

Fig. 12. Cooling kinetics of S_1 *trans*-stilbene, as indicated by the observed time dependence of the peak position of the ~1570 cm^{-1} band, in chloroform (filled circles, left axis) and in ethylene glycol (open circles, right axis). Best fitted single exponential functions are also shown. Steeper increase in ethylene glycol means faster cooling of S_1 *trans*-stilbene in this solvent than in chloroform.

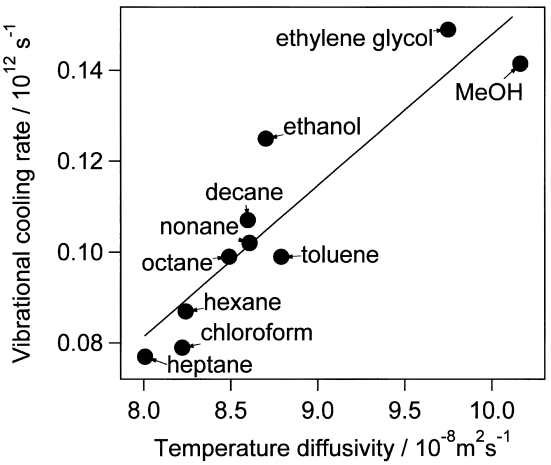

Fig. 13. Relationship between the vibrational cooling rate of S_1 *trans*-stilbene and the temperature diffusivity of the used solvent.

the excess energy is dissipated from the solute molecule into the bulk solvent, the energy should move over two types of molecular interfaces, the solute-solvent interface and the solvent-solvent interface. If the energy transfer through the solute-solvent interface is much faster than through the solvent-solvent interface, the whole transfer rate is determined by the slower solvent-solvent energy transfer rate. The rate of the solvent-solvent energy transfer process should be described well by the heat conduction in the bulk solvent, which follows the diffusion equation of heat,

$$\frac{\partial U}{\partial T} = \kappa \nabla^2 U \tag{5}$$

where U is temperature and κ is temperature diffusivity.

Based on the assumption that the solvent–solvent energy transfer determines the rate of excess energy dissipation from the solute, we have tried to explain the observed cooling kinetics by using the diffusion equation of heat (5).[38] The equation can be solved if the initial condition and the boundary condition are given appropriately. As the initial condition, we assume that, immediately after the photoexcitation (or within the 3 ps duration of the light pulse used in the experiment), the excess energy is equally distributed in a box that corresponds to the solute and nearby surrounding solvent molecules. Heat localized in this box then starts to be dissipated, following the diffusion equation (5) with the temperature diffusivity of the room temperature bulk solvent. The box is assumed to have dimensions of $(1.3 + \alpha)$ nm$\times(0.7 + \alpha)$ nm$\times(0.2 + \alpha)$ nm. The volume of 1.3 nm$\times$0.7 nm$\times$0.2 nm corresponds to the molecular volume of S_1 *t*SB and the parameter α represents additional volume for the surrounding solvent molecules that share the energy immediately after the photoexcitation. The value of α is used as a fitting parameter. For temperature diffusivity, the value reported in the literature is used throughout the analysis. As shown in Fig. 14, this model reproduces the observed cooling curve in hexane very well with the use of the temperature diffusivity value given in the literature.[68] The best fit is obtained when the parameter α is equal to 1.25 nm (Fig. 14(a)). If, however, it is assumed that the excess energy is initially localized at the coordinate origin, the model function does not reproduce the observed kinetics (Fig. 14(b)). The α value of 1.25 nm matches, at least semi-quantitatively, the thickness of the first solvation shell. This result supports our assumption that the solute–solvent energy transfer is much faster resulting in the immediate energy transfer from the solute to the nearby solvent molecules just after the photoexcitation. The apparent cooling rate of the solute is determined by

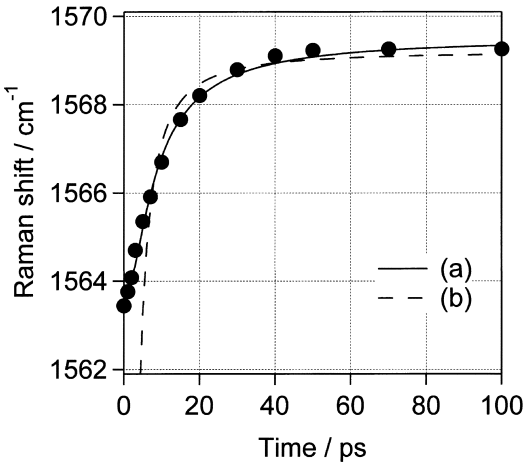

Fig. 14. Cooling kinetics of S_1 *trans*-stilbene in hexane, as indicated by measured time dependence of the peak position of the ~1570 cm^{-1} band (filled circles). The observed kinetics is interpreted by an excess energy dissipation mechanism based on the diffusion equation of heat. Simulated curves are also shown for two initial conditions, (a) the energy is initially distributed in a box with dimensions of $(1.3 + \alpha)$ nm$\times$ $(0.7 + \alpha)$ nm $\times$ $(0.2 + \alpha)$ nm, and (b) at the coordinate origin. The best fit for (a) is obtained when $\alpha = 1.25$ nm.

the solvent–solvent energy transfer and hence by the heat conduction capability of the bulk solvent.

It is possible to estimate the number of solvent chloroform molecules in the first solvation shell which accept energy efficiently from S_1 *t*SB. The initial temperature rise upon the photoexcitation in the chloroform solution is determined to be 65 K with the use of the "picosecond Raman thermometer". Because we know that the excess energy is 2800 cm^{-1} in the present system, we can calculate the expected temperature rise of S_1 *t*SB just after the photoexcitation. If we assume that all the normal vibrations of S_1 *t*SB are harmonic oscillators, the energy $E(\Delta T)$ needed for a temperature rise from T to $T + \Delta T$ is given by,

$$E(T, \Delta T) = \frac{3}{2}k\Delta T + \frac{3}{2}k\Delta T + \sum_{i=1}^{72} h\nu_i \left(\frac{1}{\exp\left(\frac{h\nu_i}{k(T + \Delta T)}\right)} - \frac{1}{\exp\left(\frac{h\nu_i}{kT}\right)} \right) \quad (6)$$

where ν_i is the frequency of the i-th normal mode and k is the Boltzmann constant. The first, second, and third terms in the equation represent contributions from the translational, rotational, and vibrational degrees of freedom. We have used the frequencies of the 72 normal modes of *t*SB in the ground state,[69] since reliable vibrational frequencies, especially those for low frequency modes, are not available for S_1 *t*SB. In Fig. 15, the calculated energy is plotted against the temperature rise from 294 K, at which temperature the experiments were performed. If the given excess energy of 2800 cm^{-1} is distributed solely among the vibrational, rotational, and translational degrees of freedom of S_1 *t*SB, temperature should increase by 140 K. In reality, however, the observed temperature rise is 65 K. Energy of only 1140 cm^{-1} is needed for increasing the temperature of *t*SB by 65 K. There is a difference of 1660 cm^{-1} between the given excess energy (2800 cm^{-1}) and the energy consumed for the observed temperature rise of S_1 *t*SB (1140 cm^{-1}). Because the only other degrees of freedom that can share the excess energy are those from the solvent, it is concluded that a portion (1660 cm^{-1}) of the initial excess energy is shared among the nearby solvent molecules instantaneously within the time resolution of the experiment. This result is fully consistent with our previous conclusion that the solute-solvent energy transfer is quite effective and that it is complete within the duration of the laser pulse (3 ps).

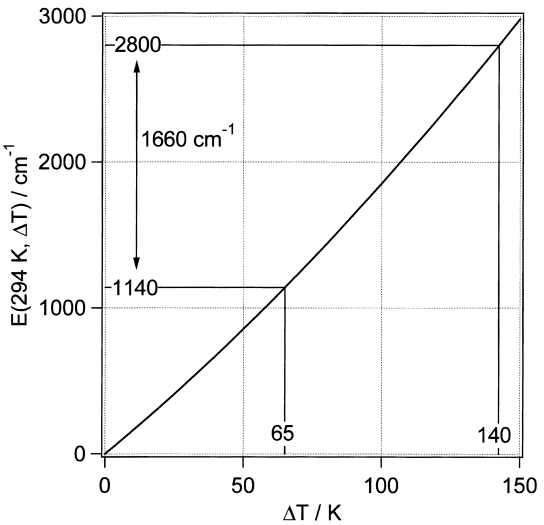

Fig. 15. Relationship between the energy (E(294 K, ΔT)) needed for increasing temperature of *trans*-stilbene by ΔT from 294 K, and ΔT.

If we assume that the temperature rise of the solvent molecules that share the excess energy is the same as that of S_1 *t*SB, we can estimate the number of the solvent molecules that accept the energy of 1660 cm^{-1}. For this calculation, we need the heat capacity of the solvent chloroform. Heat capacity of chloroform, however, is available only under the equilibrium conditions. In other words, there are no experimental data that show which of the vibrational, rotational, and translational degrees of freedom becomes or does not become statistical in a few picoseconds during the course of intermolecular energy transfer. Therefore, we calculate for the two extreme but possible cases. If all the three degrees of freedom become statistical in a few picoseconds, the number of the solvent molecules that initially share the excess energy is 4.8, because the energy acceptable by one chloroform molecule is 68 cm^{-1} for the vibrational, 68 cm^{-1} for the rotational, and 208 cm^{-1} for the rotational degrees of freedom. If, however, the energy is shared only among the translational and rotational degrees of freedom, the number should be 12. Since chloroform can move only 0.2 nm in 3 ps by normal diffusion, molecules that share the initial excess energy are most probably those contained in the first solvation shell. Thus, we estimate that, in chloroform solution of S_1 *t*SB, the number of solvent molecules in the first solvation shell is between 5 and 12.

In the excess energy dissipation process, there are two types of solvent molecules playing different roles: the solvent molecules in the first solvation shell and those in the bulk. All the solvent molecules, however, are the same chemical species and they are not distinguished with usual spectroscopic techniques. In order to chemically separate the role of the solvent in the first solvation shell and that in the bulk, we use micellar solutions. In the micelle of sodium dodecyl sulfate (SDS) aqueous solution, *t*SB is expected to be solvated in the hydrophobic part. In this system, the nearest species surrounding the solute is the dodecyl groups. Therefore, the first salvation shell consists of the dodecyl groups, whereas the bulk solvent is water. It is interesting to compare the excess energy dissipation process in this SDS micellar solution with that in dodecane, in which both the solvating and bulk species are dodecane. Picosecond fluorescence spectroscopy has revealed that the fluorescence lifetime of *t*SB in the SDS micellar solution is the same as that in the dodecane solution.[43] Since the fluorescence lifetime is a sensitive probe of the microscopic environment of S_1 *t*SB, as mentioned above, intermolecular interaction between S_1 *t*SB and the first solvation shell should be similar between the two solutions. However, the observed cooling curves in the SDS micellar solution and that in the dodecane solution are different from each other (Fig. 16).[43] Faster cooling in the micellar solution, as shown in the figure, is explained well by considering the difference between the temperature diffusivity of water (1.5×10^{-7} m^2 s^{-1} [68]) and that of dodecane. Although

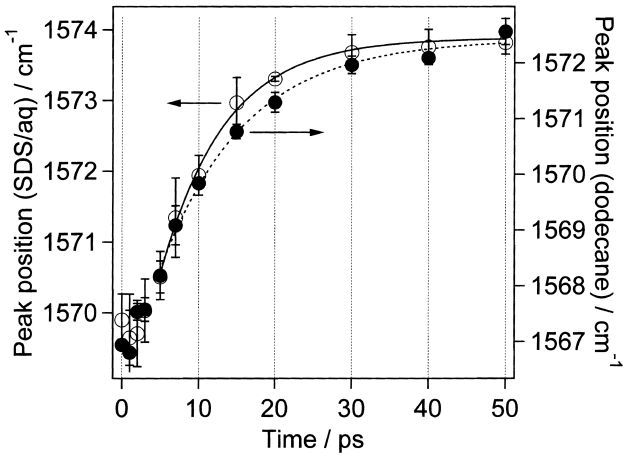

Fig. 16. Cooling kinetics of S_1 *trans*-stilbene, as indicated by the observed time dependence of the peak position of the ~1570 cm^{-1} band, in SDS micellar solution (open circles, left axis) and in dodecane (filled circles, right axis). Best fitted single exponential functions are also shown. Steeper increase in SDS micellar solution means faster cooling in this solution than in dodecane.

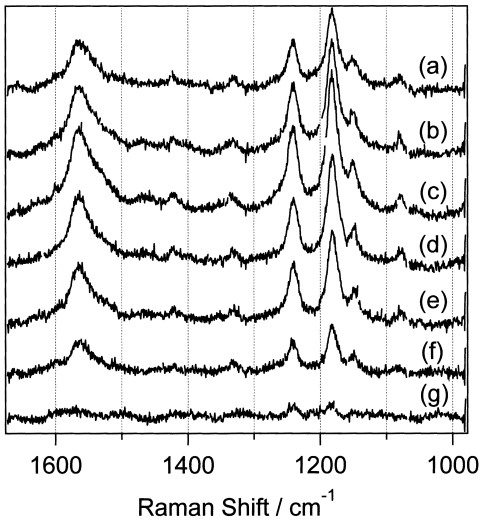

Fig. 17. Time-resolved Raman spectra of S_1 *trans*-stilbene in carbon tetrachloride measured at 0 ps (a), 1 ps (b), 3 ps (c), 5 ps (d), 7 ps (e), 10 ps (f), and 15 ps (g) after the photoexcitation.

the temperature diffusivity of dodecane is not known, it should be similar with the values for other alkanes. The temperature diffusivity of hexane, heptane, octane, nonane, and decane are 8.2×10^{-8}, 8.0×10^{-8}, 8.5×10^{-8}, 8.6×10^{-8}, and 8.6×10^{-8} m^2 s^{-1}, in this order. Because the temperature diffusivity of water should be much larger than that of dodecane, and because the entire energy dissipation rate is controlled by the heat transfer capability of the bulk solution, it is natural to have a faster cooling rate in the micellar solution than in dodecane, even if the microscopic solvation environments are similar between the two.

Thus far, we have obtained no experimental result that shows the origin of the fast solute–solvent energy transfer. Although vibration to vibration (V–V) resonance energy transfer could be an important energy transfer mechanism, there was no difference observed between the cooling kinetics in $CHCl_3$ and that in $CDCl_3$.[47]

Chlorine Abstraction of S_1 *trans*-Stilbene

In the course of our systematic study of the solvent effect on the Raman spectrum, we have found that the S_1 lifetime of *t*SB is drastically shortened in carbon tetrachloride. Time-resolved Raman spectra of *t*SB measured in carbon tetrachloride are shown in Fig. 17. Since all the Raman bands observed in the figure are assigned to S_1 *t*SB, it is obvious that the S_1 state is formed and quenched within 10 ps after the photoexcitation. Picosecond time-resolved fluorescence spectroscopy has revealed that the fluorescence lifetime of *t*SB in carbon tetrachloride is about 3 ps.[41] Although the fluorescence lifetime of *t*SB was measured in a number of solvents, the shortest lifetime ever reported was 30 ps, that in methanol and in acetonitrile. The newly found fluorescence quenching rate in carbon tetrachloride is larger than that in ordinary solvents by ten times or more.

An obvious question on this anomalous fluorescence lifetime shortening is whether or not the *trans–perpendicular* isomerization rate is accelerated by ten times or more in carbon tetrachloride. The answer for this question has been obtained by a steady-state photoirradiation experiment. When *t*SB is irradiated with near-UV light in ordinary solvents, its concentration gradually decreases while the concentration of the *cis*-isomer increases. When this process is monitored with UV absorption spectroscopy, an isosbestic point is observed at 265 nm (Fig. 18). If the same experiment is performed in car-

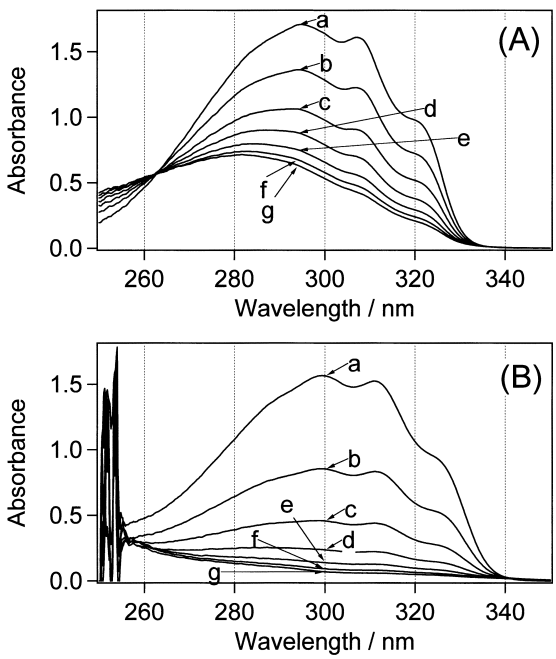

Fig. 18. UV absorption spectra of *trans*-stilbene in heptane (A) and in carbon tetrachloride (B) measured before (a) and after 5 min (b), 10 min (c), 15 min (d), 20 min (e), 25 min (f), and 30 min (g) of steady-state photoirradiation in the near-UV.

bon tetrachloride, however, there is no formation of the *cis*-isomer observed. The absorption signal for *t*SB decreases monotonically, indicating that it decomposes as a result of some unknown photochemical reactions.

Figure 18 shows that there is no distinct electronic absorption signature that is assignable to the product of the photochemical reaction of *t*SB in carbon tetrachloride. Thus, time-resolved infrared absorption spectroscopy has been used, in which a carbon tetrachloride solution of *t*SB was irradiated with the 262 nm light pulse and the induced infrared spectral changes were recorded by a highly sensitive nanosecond time-resolved infrared spectrometer.[70,71] The result is shown in Fig. 19.[41] In the figure, transient infrared absorption from newly generated species is represented by upward peaks while the depletion of the ground-state absorption is represented by downward peaks. The prominent upward peak at 896 cm^{-1} has been identified as due to the trichloromethyl (CCl_3) radical. The downward peak at 960 cm^{-1} is ascribed to the loss of the CH out-of-plane bend mode of the olefinic part of *t*SB. These results indicate that a chlorine atom is transferred from carbon tetrachloride to *t*SB upon photoexcitation, forming the *t*SB–Cl adduct and the CCl_3 radical. Time dependence of the 896 cm^{-1} band has revealed that the CCl_3 radical decays in approximately 100 μs, following the second-order decay kinetics.[41] Because the CCl_3 radical and the *t*SB–Cl adduct are formed in a single photochemical reaction and because their initial concentrations are the same, the recombination reaction should follow the second-order kinetics if it occurs after complete dissociation of the geminate pair. Recently, similar photochemical reactions with carbon tetrachloride have been shown for anthracene[72] and biphenyl,[73] based on the experimental results from nanosecond time-resolved infrared spectroscopy and picosecond time-resolved fluorescence spectroscopy. It seems general for aromatic molecules to react with carbon tetrachloride when photoexcited to the electronically excited singlet state.

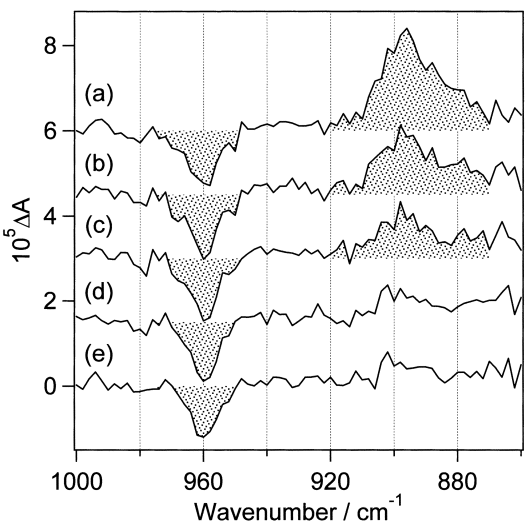

Fig. 19. Time-resolved infrared difference spectra of *trans*-stilbene in carton tetrachloride measured at 0–50 μs (a), 50–100 μs (b), 100–150 μs (c), 150–200 μs (d), and 200–250 μs (e) after the photoexcitation at 262 nm.

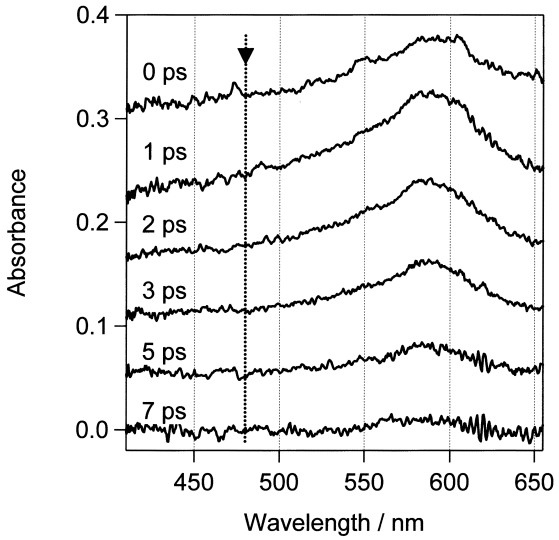

Fig. 20. Time-resolved visible absorption spectra of *trans*-stilbene in carton tetrachloride. Time dependence of the S_n–S_1 absorption is shown. Vertical line with an arrow indicates the spectral position where the absorption band from the cation radical of *trans*-stilbene is expected.

The bimolecular reaction between S_1 *t*SB and carbon tetrachloride in the picosecond time region has been traced by femtosecond time-resolved visible absorption spectroscopy.[74] In this experiment, *t*SB is photoexcited with the 266 nm light pulse and the induced absorption change in the visible region is monitored with the white light continuum generated by the self-phase modulation of the 800 nm light in water.[75] The obtained time-resolved spectra are shown in Fig. 20. Transient absorption band at 580 nm is due to the S_n–S_1 absorption of *t*SB. The characteristic absorption band of the *t*SB cation radical at 480 nm[76] is not observed in the spectra in Fig. 20. Therefore, the cation radical is not a reaction intermediate in the photochemical reaction between *t*SB and carbon tetrachloride. It is highly likely that the chlorine atom is directly transferred from carbon tetrachloride to S_1 *t*SB.

Exact kinetic behavior of the bimolecular reaction can be obtained by plotting the intensity of the S_n–S_1 absorption at 580 nm against time. The observed kinetics (Fig. 21) is explained well by the Smoluchowski theory of diffusion-controlled reactions.[77,78] According to this theory, the bimolecular reaction constant $k(t)$ can be expressed as,

$$k(t) = 4\pi R N_A D \left(1 + \frac{R}{\sqrt{\pi D t}}\right) \quad (7)$$

where D is the relative diffusion coefficient, N_A is the Avogadro number, and R is the distance between the two reactants where the reaction occurs with unit probability. The best fit to the observed reaction kinetics is obtained when R is 0.42 nm (Fig. 21). The R value calculated from the molecular volume with the filling factor of 0.740 (corresponding to the closest packing crystals) is 0.67 nm. The Collins–Kimball theory,[78,79] which assumes a finite reaction probability at the distance R, also reproduces the observed bimolecular kinetics successfully when R is 0.50 nm and the intrinsic bimolecular

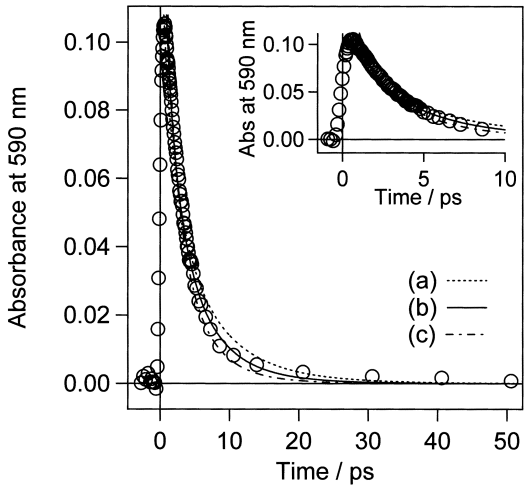

Fig. 21. Observed time profile of the S_n–S_1 absorption intensity of *trans*-stilbene in carbon tetrachloride, indicating the bimolecular reaction kinetics between S_1 *trans*-stilbene and carbon tetrachloride (open circles). The kinetics simulated by Smoluchowski's theory of diffusion-controlled reactions are also shown for R = 0.37 nm, 0.42 nm (best fit, b), and 0.47 nm (c). Early time kinetics is shown in the inset with an expanded horizontal axis.

rate constant is 7.0×10^{10} mol^{-1} dm^3 s^{-1}. Although the two theories of diffusion-controlled reactions assume that a reactant is spherically shaped and that the radial distribution of another reactant is constant, they reproduce the observed reaction kinetics quite well. If the reacting points on the *t*SB molecule are localized, rotational diffusion must contribute to the reaction kinetics. The involvement of the rotational diffusion will make the apparent R value smaller than the one expected from the space filling model. This might explain the fact that the R values obtained from the above analysis are smaller than the value estimated from the molecular volume. The diffusion-controlled reaction theory should be applied to the time region where the translational motion of the reactants is well described by diffusion. The present experimental results suggest that a time period of a few picoseconds is long enough for the molecular motion in solution to be described well by the scheme of diffusion. This conclusion is supported by a molecular dynamics simulation which shows that the velocity correlation time of carbon tetrachloride at room temperature is 0.1 to 0.2 ps.[80] Recently, similar agreement between the observed reaction kinetics and the theories of diffusion-controlled reactions has been reported for the photoinduced bimolecular reaction between biphenyl and carbon tetrachloride, which is also completed in approximately 3 ps.[81] Temperature dependence of the fluorescence lifetime of *t*SB in carbon tetrachloride has also been successfully explained by the reported temperature dependence of the diffusion coefficient of carbon tetrachloride.[82]

Concluding Remarks

The type of information obtained by the studies described here extends from the structure and dynamics of an electronically excited molecule in solution to a new view on the photoisomerization reaction, from a microscopic picture of the solvent-solute interaction to a new photochemical reaction in carbon tetrachloride. We owe this wealth of new molecular information to S_1 *t*SB and time-resolved Raman spectroscopy.

It is a great pleasure and honor for the present authors to compile their decadal Raman spectroscopic investigations of S_1 *trans*-stilbene as an Account of the Bulletin of the Chemical Society of Japan. They are grateful to Professor Renji Okazaki, the Editor of the Bulletin, for this opportunity. They also express their sincere gratitude to all the collaborators of the work described in this Account.

References

1 J. Saltiel, J. D'Agostino, E. D. Magarity, L. Metts, K. R. Neuberger, M. Wrighton, and O. C. Zafirou, *Org. Photochem.*, **3**, 1 (1971).
2 R. M. Hochstrasser, *Pure Appl. Chem.*, **52**, 2683 (1980).
3 D. H. Waldeck, *Chem. Rev.*, **91**, 415 (1991).
4 G. H. Atkinson, "Advances in Infrared and Raman Spectroscopy," ed by R. J. H. Clark and R. E. Hester, Heyden, London (1982), Vol. 9.
5 H. Hamaguchi, "Vibrational Spectra and Structure," ed by J. R. Durig, Elsevier, Amsterdam (1987), Vol. 16, p. 227.
6 H. Hamaguchi and T. L. Gustafson, *Ann. Rev. Phys. Chem.*, **45**, 593 (1994).
7 T. L. Gustafson, D. M. Roberts, and D. A. Chernoff, *J. Chem. Phys.*, **79**, 1559 (1983).
8 H. Hamaguchi, C. Kato, and M. Tasumi, *Chem. Phys. Lett.*, **100**, 3 (1983).
9 H. Hamaguchi, T. Urano, and M. Tasumi, *Chem. Phys. Lett.*, **106**, 153 (1984).
10 T. L. Gustafson, D. M. Roberts, and D. A. Chernoff, *J. Chem. Phys.*, **81**, 3438 (1984).
11 H. Hamaguchi, *J. Mol. Struct.*, **126**, 125 (1985).
12 J. B. Hopkins and P. M. Rentzepis, *Chem. Phys. Lett.*, **124**, 79 (1986).
13 S. A. Payne and R. M. Hochstrasser, *J. Phys. Chem.*, **90**, 2068 (1986).
14 H. Hamaguchi, *Chem. Phys. Lett.*, **126**, 185 (1986).
15 T. L. Gustafson, D. A. Chernoff, J. F. Palmer, D. M. Roberts, "Time-resolved Vibrational Spectroscopy," ed by G. H. Atkinson, Gordon and Breach, New York (1987), p. 265.
16 H. Hamaguchi, "Time-resolved Vibrational Spectroscopy," ed by G. H. Atkinson, Gordon and Breach , New York (1987), p. 320.
17 V. F. Kamalov, N. I. Koroteev, A. P. Shkurinov, and B. N. Toleutaev, *Chem. Phys. Lett.*, **147**, 335 (1988).
18 H. Hamaguchi, *J. Chem. Phys.*, **89**, 2587 (1988).
19 V. F. Kamalov, N. I. Koroteev, B. N. Toleutaev, A. P. Shkurinov, and U. Stamm, *J. Phys. Chem.*, **93**, 5645 (1989).
20 V. F. Kamalov, N. I. Koroteev, A. P. Shkurinov, and B. N. Toleutaev, *J. Mol. Struct.* **217**, 19 (1990).
21 K. Iwata and H. Hamaguchi, *Chem. Phys. Lett.*, **196**, 462 (1992).
22 W. L. Weaver, L. A. Huston, K. Iwata, and T. L. Gustafson, *J. Phys. Chem.*, **96**, 8956 (1992).
23 K. Iwata, W. L. Weaver, and T. L. Gustafson, *Chem. Phys. Lett.*, **210**, 50 (1993).
24 H. Hamaguchi and K. Iwata, *Chem. Phys. Lett.*, **208**, 465 (1993).

25 R. E. Hester, P. Matousek, J. N. Moore, A. W. Parker, W. T. Toner, and M. Yowire, *Chem. Phys. Lett.*, **208**, 471 (1993).
26 J. Qian, S. L. Schultz, G. R. Bradburn, and J. M. Jean, *J. Phys. Chem.*, **97**, 10638 (1993).
27 K. Iwata, S. Yamaguchi, and H. Hamaguchi, *Rev. Sci. Instrum.*, **64**, 2140 (1993).
28 K. Iwata, B. N. Toleutaev, and H. Hamaguchi, *Chem. Lett.*, **1993**, 1603.
29 A. P. Shkurinov, N. I. Koroteev, G. Jonusauskas, and C. Rulliere, *Chem. Phys. Lett.*, **223**, 573 (1994).
30 J. Qian, S. L. Schultz, G. R. Bradburn, and J. M. Jean, *J. Lumin.*, **60–61**, 727 (1994).
31 H. Okamoto, T. Nakabayashi, and M. Tasumi, *J. Raman Spectrosc.*, **25**, 631 (1994).
32 J. Qian, S. L. Schultz, and J. M. Jean, *Chem. Phys. Lett.*, **223**, 9 (1995).
33 P. Matousek, A. W. Parker, W. T. Toner, M. Towire, D. L. A. de Faria, R. E. Hester, and J. N. Moore, *Chem. Phys. Lett.*, **237**, 373 (1995).
34 K. Iwata and H. Hamaguchi, *J. Mol. Liq.*, **65/66**, 417 (1995).
35 M. Towire, P. Matousek, A. W. Parker, W. T. Toner, and R. E. Hester, *Spectrochim. Acta, A*, **51**, 2491 (1995).
36 J. Oberle, E. Abraham, A. Ivanov, G. Jonusauskas, and C. Rulliere, *J. Phys. Chem.*, **100**, 10179 (1996).
37 V. Deckert, K. Iwata, and H. Hamaguchi, *J. Photochem. Photobiol., A*, **102**, 35 (1996).
38 K. Iwata and H. Hamaguchi, *J. Phys. Chem. A*, **101**, 632 (1997).
39 S. L. Schultz, J. Qian, and J. M. Jean, *J. Phys. Chem.*, **101**, 1000 (1997).
40 T. Nakabayashi, H. Okamoto, and M. Tasumi, *J. Phys. Chem. A*, **101**, 7189 (1997).
41 K. Iwata and H. Hamaguchi, *Bull. Chem. Soc. Jpn.*, **70**, 2677 (1997).
42 T. Nakabayashi, H. Okamoto, and M. Tasumi, *J. Phys. Chem. A*, **102**, 9686 (1998).
43 K. Iwata and H. Hamaguchi, *J. Raman Spectrosc.*, **29**, 915 (1998).
44 H. Hamaguchi, *Acta Phys. Pol., A*, **95**, 37 (1999).
45 T. Nakabayashi, H. Okamoto, and M. Tasumi, *Laser Chem.*, **19**, 75 (1999).
46 H. Okamoto, T. Nakabayashi, and M. Tasumi, *Laser Chem.*, **19**, 335 (1999).
47 K. Iwata and H. Hamaguchi, *Laser Chem.*, **19**, 367 (1999).
48 H. Okamoto, T. Nakabayashi, and M. Tasumi, *J. Raman Spectrosc.*, **31**, 305 (2000).
49 K. Iwata, *Bull. Chem. Soc. Jpn.*, in press.
50 F. W. Langkilde, R. Wilbrandt, F. Negri, and G. Orlandi, *Chem. Phys. Lett.*, **165**, 66 (1990).
51 F. W. Langkilde, R. Wilbrandt, A. M. Brouwer, F. Negri, F. Zerbetto, and G. Orlandi, *J. Phys. Chem.*, **98**, 2254 (1994).
52 J. Saltiel, *J. Am. Chem. Soc.*, **89**, 1036 (1967).
53 G. Orlandi and W. Siebrand, *Chem. Phys. Lett.*, **30**, 352 (1975).
54 See for example, J. Troe and K.-M. Weitzel, *J. Chem. Phys.*, **88**, 7030 (1988), and references therein.
55 J. M. Hicks, M. T. Vandersall, E. V. Sitzmann, and K. B. Eisenthal, *Chem. Phys. Lett.*, **135**, 413 (1987).
56 C. L. Schilling and E. F. Hilinski, *J. Am. Chem. Soc.*, **110**, 2296 (1988).
57 M. Tasumi, T. Urano, and H. Hamaguchi, "Time-resolved Vibrational Spectroscopy," ed by G. H. Atkinson, Gordon and Breach , New York (1987), p. 252.
58 A. Warshel, *J. Chem. Phys.*, **62**, 214 (1975).
59 F. Negri, G. Orlandi, and F. Zerbetto, *J. Phys. Chem.*, **93**, 5124 (1989).
60 K. Iwata and H. Hamaguchi, "Time-resolved Vibrational Spectroscopy," ed by A. Lau, F. Siebert, and W. Werncke, Springer-Verlag, Berlin (1994), p. 85.
61 P. W. Anderson, *J. Phys. Soc. Jpn.*, **9**, 316 (1964).
62 R. M. Shelby, C. B. Harris, and P. A. Cornelius, *J. Chem. Phys.*, **70**, 34 (1979).
63 H. Hamaguchi, *Mol. Phys.*, **89**, 463 (1996).
64 K. Iwata, R. Ozawa, and H. Hamaguchi, *J. Phys. Chem. A*, in press.
65 T. Hayashi and H. Hamaguchi, *Chem. Phys. Lett.*, **326**, 115 (2000).
66 G. Rothenberger, D. K. Negus, and R. M. Hochstrasser, *J. Chem. Phys.*,**79**, 5360 (1983).
67 S. K. Kim, S. H. Courtney, and G. R. Fleming, *Chem. Phys. Lett.*, **159**, 543 (1989).
68 Y. S. Touloukian, P. E. Liley, S. C. Saxena, "Thermal Conductivity, Nonmetallic Liquids and Gases," The TPRC Data Series, Thermophysical Properties of Matter Vol. 3, IFI/Plenum Data Corporation, New York (1970).
69 T. Urano, Thesis for Dr. Sci., The University of Tokyo (1990).
70 K. Iwata and H. Hamaguchi, *Appl. Spectrosc.*, **44**, 1431 (1990).
71 T. Yuzawa, C. Kato, M. W. George, and H. Hamaguchi, *Appl. Spectrosc.*, **48**, 684 (1994).
72 K. Iwata and H. Hamaguchi, *J. Mol. Struct.*, **413-414**, 101 (1997).
73 K. Iwata and H. Takahashi, *J. Mol. Struct.*, **598**, 97 (2001).
74 K. Iwata and H. Hamaguchi, *Chem. Lett.*, **2000**, 456.
75 S. Yamaguchi and H. Hamaguchi, *Chem. Phys. Lett.*, **227**, 225 (1994).
76 T. Shida and W. H. Hamill, *J. Chem. Phys.*, **44**, 2375 (1966).
77 M. v. Smoluchowski, *Z. Phys. Chem.*, **92**, 129 (1917).
78 S. A. Rice, "Diffusion-limited reactions," Comprehensive chemical kinetics 25, ed by C. H. Bamford, C. F. H. Tipper, and R. G. Compton, Elsevier, Amsterdam, (1985).
79 F. C. Collins and G. E. Kimball, *J. Colloid Sci.*, **4** , 425 (1949).
80 O. Steinhauser and M. Neumann, *Mol. Phys.*, **40**, 115 (1980).
81 K. Iwata, S. Takeuchi, and T. Tahara, *Chem. Phys. Lett.*, **347**, 331 (2001).
82 K. Iwata and H. Hamaguchi, *Chem. Phys. Lett.*, **261**, 208 (1996).

Hiro-o Hamaguchi, Professor at the Department of Chemistry, School of Science, the University of Tokyo, was born on September 21, 1947. He graduated from The University of Tokyo in 1970 and obtained the degree of Doctor of Science in 1975 under the supervision of Professor Takahiko Shimanouchi. Since then he worked as a faculty (Research Associate, Lecturer, Associate Professor) of the Department of Chemistry until 1990 when he moved to the Kanagawa Academy of Science and Technology. During 1977–1979 he was a Ramsay Fellow working with Professor A. D. Buckingham at the Department of Theoretical Chemistry, Cambridge University, UK. Since 1995, he has been Professor at The University of Tokyo (1995–1997, Graduate School of Arts and Sciences; 1997–, School of Science). He is interested in looking into *the wonder world of molecules* by spectroscopy, particularly by vibrational spectroscopy. His recent research activities include development of new spectroscopic methods, ultrafast molecular processes in solution, properties of ionic liquids and physical chemistry of living cells.

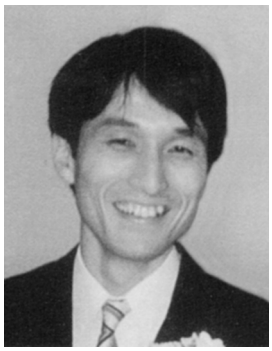

Koichi Iwata, Associate Professor, Research Centre for Spectrochemistry, School of Science, The University of Tokyo, was born in 1961. He graduated from Department of Chemistry, School of Science, The University of Tokyo in 1984. He joined Prof. Tasumi's group as a graduate student and received his Dr. Sci. degree from The University of Tokyo in 1989. He then joined Prof. Gustafson's group at Department of Chemistry, The Ohio State University, USA, as a postdoctoral fellow. In 1991, he joined Prof. Hamaguchi's group at Kanagawa Academy of Science and Technology (KAST) as a research associate. After serving as Visiting Research Associate Professor, Advanced Research Institute for Science and Engineering, Waseda University, he joined Department of Chemistry, School of Science, The University of Tokyo as an associate professor in 1997. He moved to the present institute at 2001. He is Visiting Associate Professor of Institute for Molecular Science. His research interests include development of molecular spectroscopic methods as well as studying time-dependent phenomena, in particular dynamic processes accompanying chemical reactions in condensed phases.